

Flame Spread in Laminated Bamboo Structures

Solarte A.^{1,*}, Numapo J.¹, Hidalgo J.P.¹, Torero J.L.²

¹ *The University of Queensland, Brisbane, Australia*

² *University of Maryland, Maryland, USA*

*Corresponding author's email: a.solartecastaneda@uq.edu.au

ABSTRACT

Flame spread behaviour of laminated bamboo produced from the species *Phyllostachys pubescens* (Moso) is characterised herein by determining relevant properties such as thermal conductivity and thermal inertia, which ultimately are correlated with the flame spread rate of the material. A description of the variance of thermal conductivity at temperatures ranging from ambient to 350°C is provided in order to accurately account for possible charring and heat transfer processes taking place at the surface of the samples. Testing for those thermal properties was carried out for both parallel and perpendicular positions of the fibre relative to the heat source. For the actual flame spread characterisation, the theory and methodology associated with the Lateral Ignition and Flame Spread Test (LIFT) apparatus was followed. Piloted ignition and opposed flame spread in lateral configuration framework are used for analysis, making possible to obtain the parameters of the progressed distance of the flame, maximum travelled distance, effective spread and time for extinction. In the same manner, the Flame Spread Parameter, a value that can be used for material classification, is calculated using the thermal inertia of the material at ambient and elevated temperatures. The values obtained for flame spread velocity did not adhere to a specific trend; this condition is possibly due to the formation of cracks and a charring front in the sample surface during preheating.

KEYWORDS: Flame spread, thermal inertia, thermal conductivity, flame spread parameter.

NOMENCLATURE

V_f	spread rate (m/s)	q_g''	heat transfer through gas (W/m ²)
k	thermal conductivity (W/mK)	$q_{o,ig}''$	critical heat flux for ignition (W/m ²)
C_p	specific heat capacity (J/kgK)	h_T	heat transfer coefficient (W/m ² K)
T_{ig}	Temperature for ignition (°C)		
T_s	Surface temperature (°C)		
q_e''	external heat flux (W/m ²)		
q_s''	heat transfer through the solid (W/m ²)		

Greek

ϕ flame spread parameter (kW²/m³)

Subscripts

∞ ambient

INTRODUCTION

Today's society is competing to build the tallest buildings with the latest technological designs, all in the most sustainable way. This reality drives us to pick the most innovating materials that would allow to design and construct those structures. Engineered-bamboo products are novel construction materials currently being used by engineers and architects in buildings [1]. Its favourable qualities include features such as great aesthetics, environmentally renewable and sustainable nature [2, 3],

Proceedings of the Ninth International Seminar on Fire and Explosion Hazards (ISFEH9), pp. 755-766

Edited by Snegirev A., Liu N.A., Tamanini F., Bradley D., Molkov V., and Chaumeix N.

Published by Saint-Petersburg Polytechnic University Press

ISBN: 978-5-7422-6498-9 DOI: 10.18720/spbpu/2/k19-125

excellent mechanical properties [4] with favourable structural behaviour that has shown to be equal to or greater than timber, and because of this it is being used in many regions of the world [5]. All of these characteristics contribute to place bamboo as an innovative construction material with a great potential to be used in structural elements, internal lining and external façade for modern multi-story buildings.

RESEARCH SIGNIFICANCE

Despite the positive qualities described above, the fire hazard is an important matter that needs to be addressed. Currently, there is limited knowledge related to the flame spread behaviour of this material. Recent events like the fires in the Grenfell Tower in London and Sao Paulo's high-rise building collapse are a consequence of the little information available on the characterisation of the flame spread behaviour in novel materials and complex systems.

To date, previous research has provided information on flame spread modelling of PMMA and other ideal materials from the point of view of pyrolysis and combustion. However, the existing models addressing cellulosic, charring and composites materials are much more limited and generally difficult to implement in practice [6].

The understanding of the fire spread phenomena needs to be looked in a holistic way, and the ability to tackle the problem from its basic principles is fundamental. Only once this knowledge is obtained, a trained professional will be able to assess and design fire-safe structures that take in consideration the full-scale fire scenario, which is key to create solutions to the problem thoroughly. The use of experiments like the Lateral Ignition and Flame Spread Test (LIFT) provides flammability parameters that describe the heat transfer mechanism from the flame to the fuel, which can be incorporated into mathematical correlations that will characterise the velocity of the flame spread [7]. The information from these fundamental studies provides input data for assessing risks in a real fire scenario. It is important to understand that the parameters obtained by these tests are not material properties, but a combination of the specific conditions and configurations by which the samples are tested [8]. For example, changes in natural convection, atmospheric conditions, or moisture content, among others, can cause particular behaviours. Therefore, the extrapolation to different scenarios needs to be done with caution.

This work is part of an ongoing project that intends to characterise the fire performance of laminated bamboo by exploring the flame spread parameter. The characterisation of how the flame spreads will provide an understanding on how the fire will grow and its contribution to the production of the smoke and heat influencing the occurrence of flashover in a compartment, or the external flame spread in a façade system. This information constitutes a tool for performance-based design approach that is necessary to build future fire-safe bamboo buildings.

METHODOLOGY

Materials and Methods

The present study will provide the flame spread characterisation of three different samples of laminated bamboo *Phyllostachys pubescens* (Moso). This experimental programme consists of two main steps of testing. The first step comprises bench-scale tests of laminated bamboo samples to determine their thermal conductivity and obtain the thermal inertia. The second step aims to provide information about the flame spread parameters of the same material. For this work, three different types of laminated bamboo were tested. Table 1 describes each of the samples.

Thermal properties

The thermal inertia is the resistance of a material to change its temperature, and it is a key parameter to characterise the flame spread. It is the product of the thermal conductivity, k (W/(m·K)), the density ρ (kg/m³) and the specific heat capacity, C_p (J/(kg·K)). The thermal conductivity is a parameter that drives a material's ability to conduct heat, and determines the rate at which energy is transported. The thermal conductivity will depend and change according to its physical structure, as well as its atomic and molecular characteristics [9].

Table 1. Types of laminated bamboo “Moso” tested

Laminates bamboo	Adhesive	Treatment	Use	Density, kg/m ³	Moisture Content, %
Sample A	Polyurethane	Not Steamed	Interior	540	7.17%±0.06
Sample B	Resorcinol Formaldehyde	Steamed	Interior	730	6.08%±0.40
Sample C	Formaldehyde Preferere	Steamed	Intended for structural applications	745	8.12%±0.02

Due to the process of fabrication of the laminated bamboo (hot-pressing, bleaching, caramelising, type of adhesive, etc.) [10], some physical characteristics could be changed and different values of thermal conductivity might be obtained from different manufacturing process. According to Fernandez-Pello et al. [11], the difference in thermal conductivity can affect the way that heat is transferred in the solid, and a sample comprised by high conductive materials would result in a high rate for the flame spread. This property is also key to characterise the mechanical behaviour in fire conditions due to the way in which heat transfer will take place.

The thermal conductivity was measured experimentally with the use of the Hot Disk Thermal Constants Analyser, which uses the transient plane source (TPS) method. This process is based on the use of a transiently heated plane sensor, that conducts electrical impulses in a double spiral pattern [12]. This sensor was fitted in between two sample pieces and through the application of an electrical current, the temperature of the sensor was increased and the resistance temperature was recorded as a function of time [13].

Three types of samples mentioned in Table 1, were analysed. Samples B and C were tested at the three surface sides of a cubic sample. As shown in Fig. 1, side PP1 and PP2 is the nomenclature used for the surface that is exposed perpendicularly to the fibre and side PLL refers to the surface that has been exposed parallel to the fibre. The difference between PP1 and PP2 is that PP1 has the long side of the strip (around 6 mm) placed horizontally, and PP2 has the long side of the strip placed vertically. These tests were conducted for ambient conditions (20°C -25°C) as well as for elevated temperatures (50°C - 350°C). For ambient tests, the sensor spiral was sandwiched between two sheets of Kapton, and for the elevated temperatures two sheets of Mica was used.

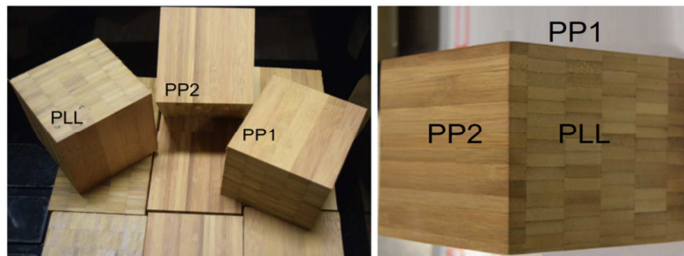


Fig. 1. Nomenclature of the surface tested on the laminated bamboo samples.

Flame spread

Flame spread is a mechanism in which a flame moves forward in the proximity of a pyrolysing region of the surface fuel [6]. When studying flame spread behaviour, it is important to assess the governing mechanisms of the material that can influence the phenomenon such as configuration, thickness and intrinsically material characteristics such as thermal inertia, thermal conductivity, melting, charring, delamination, among others [11]. Previous studies have analysed the different behaviour of flame spread, however, two principle modes have been established: (1) opposed-flow flame spread and (2) concurrent flow flame spread [11].

From Fig. 2a, it can be seen that for opposed-flow flame spread, the flame front is moving forward, preheating the unburned fuel. However, there is a flow coming from the opposite direction which may or may not slow down the movement of the flame, according to the de Ris regime [14], or Fernandez-Pello regime [11]. From Fig. 2b, it can be seen how the flow is pushing in the same direction as the flame, effectively “driving” it forward and enabling propagation.

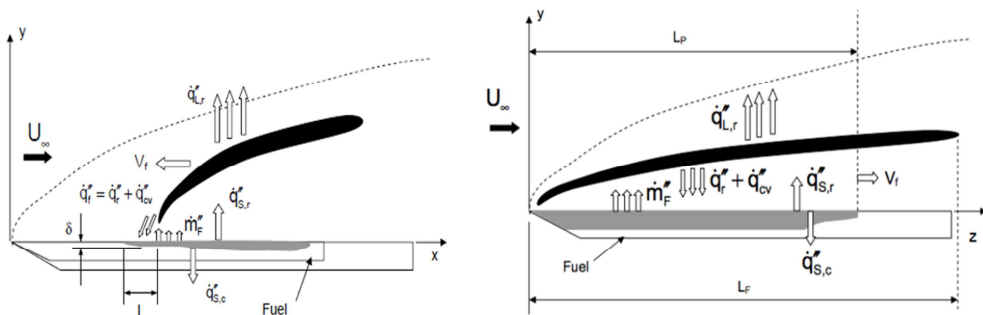


Fig. 2. (a) Opposed flow flame spread (b) concurrent flow flame spread (from Jose L. Torero class notes, University of Edinburgh, 2011).

This work will focus on the analysis of opposed flame spread in a lateral configuration, as the first step to understand the problem and classify the product. Future steps will study the vertical configuration for concurrent flow flame spread, to understand the hazards of putting this material in walls and façades. From Quintiere [15] Eq. (1) was used for the fundamentals of this study. This expression correlates the spread rate, V_f (m/s), with the thermal conductivity, k (W/(m·K)), the density ρ (kg/m³), the specific heat C_p (J/(kg·K)), the temperature for ignition T_{ig} (°K), and the surface temperature T_s (°K), and introduces the flame spread parameter, ϕ (W²/m³). The flame spread parameter is the product of heat flux from the flame onto the sample in the gas phase, and the heated length, it can be calculated experimentally with the use of the Lateral Ignition and Flame Test (LIFT).

$$V_f = \frac{\phi}{k\rho C_p (T_{ig} - T_s)^2}, \tag{1}$$

Nevertheless, to use this simplified equation, some assumptions need to be stated [8, 16, 17]:

1. The solid is considered inert until ignition.
2. T_{ig} can be used as the temperature for pyrolysis T_p .
3. Samples are thermally thick.

4. The flame is driven by three sources of heat: (1) external heat transfer (\dot{q}_e''), (2) heat transfer through the solid (\dot{q}_s''), and (3) the heat is transferred from the flame through the gas phase (\dot{q}_g''), mainly through conduction.
5. As the flame moves forward the “virgin material” reaches ignition temperature, and the flame acts as a pilot ignitor that enables the spread.
6. The flame is not close to extinction, so the heat produced is bigger than the heat needed to increase the temperature of the new air allowing the flame to spread with the thermal wave.

If the sample is preheated and achieves thermal equilibrium, the total losses of the sample are equivalent to the heat input. With this, Eq. (2), (3) and (4) are introduced to simplify Eq. (1)

$$T_{ig} = T_{\infty} + \frac{\dot{q}_{0,ig}''}{h_r}, \quad T_s = T_{\infty} + \frac{\dot{q}_e''}{h_r} \quad (2, 3)$$

and

$$T_{ig} - T_s = \frac{\dot{q}_{0,ig}'' - \dot{q}_e''}{h_r}, \quad (4)$$

where $\dot{q}_{0,ig}''$ (W/m^2) is the critical heat flux for ignition, and Eq. (5) becomes the correlation of the flame spread parameter in terms of the critical heat flux for ignition and the external heat flux applied.

$$V_f = \frac{h_r^2 \phi}{k\rho C_p (\dot{q}_{0,ig}'' - \dot{q}_e'')^2}. \quad (5)$$

Samples of *Phyllostachys pubescens* (Moso) of 600 x100 x 40 mm were studied under the Lateral Ignition and Flame Test (LIFT) based on ASTM-E-1321-13 [18]. To reduce the heat losses from the back of the sample, the sides and back of each specimen were covered by two layers of ceramic insulation material 2.5 mm thick and a final layer of aluminium foil 0.2 mm thick. The samples were placed in a holder frame angled at 15 degrees to the centreline of the radiant panel. Each sample was marked every 25 mm for tracking the movement of the flame and a video camera was placed perpendicular to the sample, to record all tests. To guarantee that the tests would start under steady thermal conditions, eight thermocouples were placed in the sample, 2 mm from the surface to follow and measure the increase of the temperature due to the heating of the surface during the arrival of the flame front.

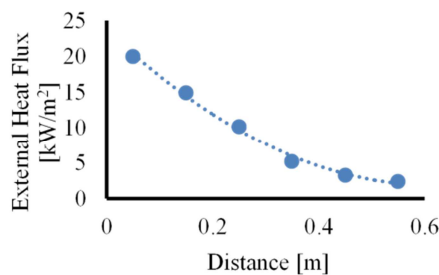


Fig. 3. Heat flux mapping distribution

Before these tests were carried out, it was mapped the external heat flux imposed from the radiant panel on the whole surface of the samples. A non-combustible fibre block was placed and the

mapping was performed starting from the leading edge at 50, 150, 250, 350, 450, and 550 mm. A water-cooled heat flux gauge was used to record the surface heat flux of each location; this it was placed around 5 mm offset of the insulation surface to avoid convection effects. A heat flux distribution is shown in Fig. 3, which was obtained by recording measurements in different locations and interpolating the values in between.

The external heat flux imposed at the leading edge was chosen to be 20 kW/m², around 5 kW/m² above the critical heat flux for ignition, which was found to be 14 kW/m² in previous experiments [19]. In order to guarantee thermal equilibrium, each sample was preheated for at least 1,000 seconds. When the temperature measured by the thermocouples reached a plateau, the sample was deemed to be reach a steady state. Once the thermal equilibrium of the specimen was reached, a pilot flame was introduced in the leading edge to mark the onset of ignition. However, given the charring nature of the material, this preheating time led to the creation of an initial charred surface in the first 150 mm of the sample before ignition occurred. Once ignition started, visual observations recorded the flame front position as a function of time. The rate at which the flame spreads will depend on the chemical decomposition and pyrolysis front that will start to progress with the ignition of the sample.

RESULTS AND DISCUSSION

Thermal inertia

To experimentally obtain the value of the thermal inertia, the thermal conductivity was measured by testing 35 samples with the Hot Disk, for ambient temperature. Sample types A, were tested for face PP1, and B and C were tested for each face PP1, PP2, PLL, the sides described in the previous section. Table 2 shows the results obtained for the thermal inertia at ambient conditions.

Table 2. Thermal conductivity and thermal inertia results of laminated bamboo “Moso” tested

Laminates bamboo at 20°C	Thermal Conductivity, W/(m·K)	Thermal Inertia, W ² ·s/(m ⁴ ·K ²)
Sample A: perpendicular to the fibre Side PP1	0.201±0.01	2.56 x10 ⁵ ±6.95 x10 ³
Sample B: perpendicular to the fibre Side PP1	0.24±0.01	3.94 x10 ⁵ ±9.50 x10 ³
Sample B: perpendicular to the fibre Side PP2	0.26±0.01	4.27 x10 ⁵ ±6.01 x10 ³
Sample B: parallel to the fibre Side PLL	0.29±0.01	4.71 x10 ⁵ ±1.47x10 ⁴
Sample C: perpendicular to the fibre Side PP1	0.25±0.01	4.13 x10 ⁵ ±2.09 x10 ⁴
Sample C: perpendicular to the fibre Side PP2	0.24±0.01	4.10 x10 ⁵ ±2.07 x10 ⁴
Sample C: parallel to the fibre Side PLL	0.27±0.01	4.44 x10 ⁵ ±1.22 x10 ⁴

The results show that the thermal conductivity tested in face PP1 for sample A is lower than for samples B and C, this can be explained due to the lower density associated with a higher porous media found for samples type A. Sample B and C show higher values for the side where the heat is transferred parallel to the grain (PLL). Sample B depicts the highest values for the sides PP2 and PLL. To obtain the thermal inertia, the values of the experimental thermal conductivity, density and specific heat were multiplied. The value of the specific heat was used as 2260 J/(kg·K), which was obtained by Bartlett et al. [20]. The highest value of the thermal inertia was found to be 4.71x10⁵ W²·s/(m⁴·K²) for sample B followed by 4.44 x 10⁵ W²·s/(m⁴·K²) by sample C, both for parallel to the grain (PLL) configuration. From Table 2 it can be seen that the values of the thermal inertia for sample A are almost 50% less than the highest value. The difference in the values obtained for sample B and C is up to 16%.

For temperatures above 30 °C test were conducted in a furnace and the thermal conductivity was measured. Sample type A, B and C were tested for two surfaces PP1 and PLL. Figure 4 shows the thermal conductivity results at elevated temperatures. For all three cases, the thermal conductivity shows higher results than those measured at ambient temperature. As for ambient temperatures, the values of sample B and C are higher than the ones obtained for Sample A. For the tests conducted perpendicular to the grain (PP1), the thermal conductivity shows a steady tendency up to around 225 °C, however, starts to decrease after the samples were heated beyond 225 °C. Samples A and B show a clear rise in the values for the tests performed parallel to the grain (PLL) in comparison to the ones perpendicular to the grain (PP1), and show higher values than the results obtained for sample C. The reduction of the thermal conductivity after 225 °C can be due to the fact that, at these temperatures, the degradation reactions trigger mass loss and charring processes which create gaps of air within the sample, resulting in a porous media and therefore lower values of thermal inertia.

For the test run perpendicular to the grain (PP1), the results from 30 to 225 °C were averaged to obtain a bulk value for this range of temperatures. The thermal conductivity for samples A, B and C were 0.26 ± 0.01 , 0.34 ± 0.01 and 0.36 ± 0.01 W/(m·K) respectively. Measurements of thermal conductivity parallel to the grain yielded the highest value of 0.38 W/mK for sample A at 84 °C, 0.47 W/(m·K) for sample B at 120 °C, and 0.43 W/(m·K) for sample C at 220 °C.

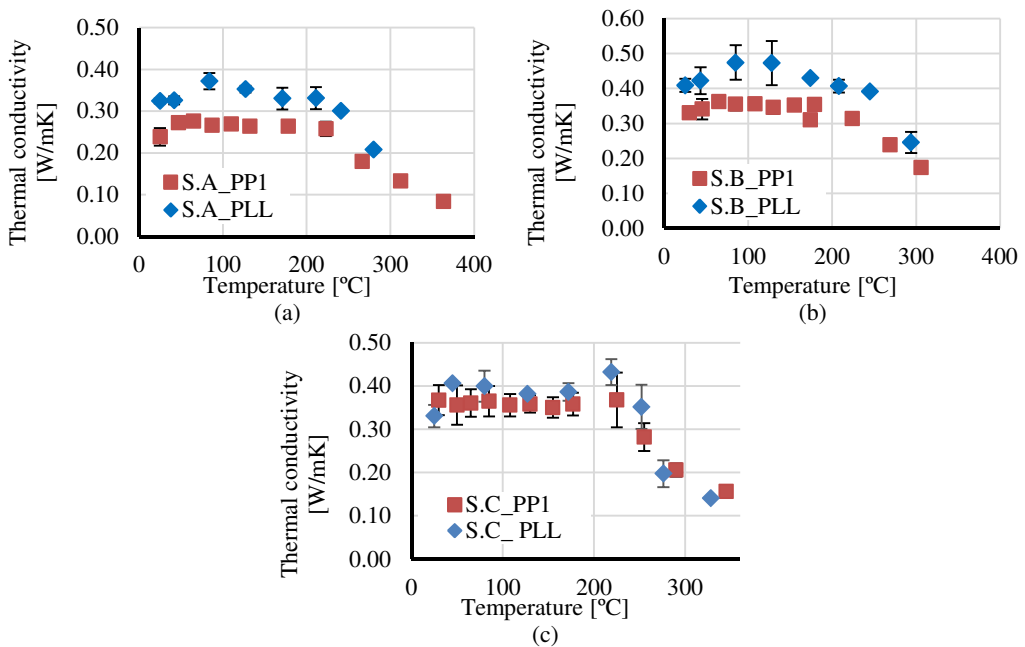


Fig. 4. Thermal conductivity at elevated temperatures (a) Sample A, (b) Sample B, (c) Sample C.

Shah et al. [21] tested samples of engineered bamboo at ambient temperatures and obtained a thermal conductivity of 0.2 ± 0.07 W/(m·K) for laminated bamboo (Moso). Compared to engineered timber, which has a thermal conductivity of 0.14 W/(m·K) [20], laminated bamboo has a higher value. To the knowledge of the authors, there was no information available to compare for this parameter at elevated temperatures.

Flame spread

Tests were carried out in the LIFT to study the flame spread behaviour of laminated bamboo. Three test were conducted for sample type B and sample type C, all exposed to the PP1 side. As shown in

Fig. 5a, the preheating caused degradation and charring of the surface of the sample for approximately 250 mm from the leading edge, therefore the readings of the flame spread started around the 250 mm mark. Figures 5b and 5c show the evolution of the travelling flame, and Fig. 5d show extinction of the flame at around 400-415 mm.

The nomenclature in the following figures indicates the sample type by S.B or S.C (sample type B or C) and the test number by T1, T2, and T3.

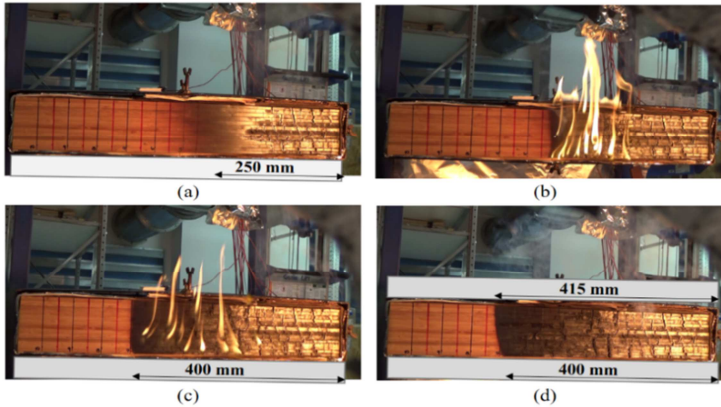


Fig. 5. Flame spread test (a) before ignition, (b) flame travelling, (c) before extinction, (d) at extinction.

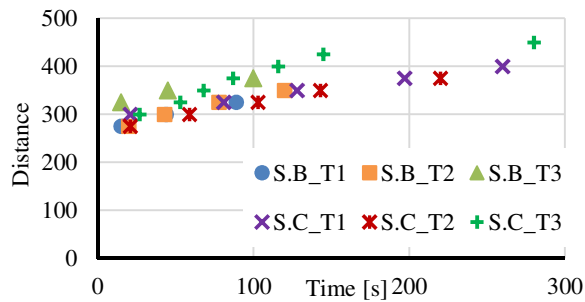


Fig. 6. Flame spread test distance travelled in time.

From Fig. 3 we can derive that the critical heat flux for flame spread was around 5 kW/m^2 . Figure 7 shows the velocity of the spread in time. Sample type B depicts a decreasing tendency with a polynomial fit. For Sample C, shown in Fig. 7b, the velocities show that they tend to decrease, slightly increase and decrease again. All samples have a similar behaviour between them but from 60 – 90 s the spread velocities of S.C_T3, increase abruptly. This could be explained because during this part of the test, it was seen an incoming flow current, possible by an open door in the lab, and seemed to have been changing the flow creating a faster and more turbulent flame. During the tests, it was possible to notice the role that the cracks and the char layer had on the spread, stopping the movement forward until the flame was able to advance. Because of this condition, no steady spread was observed.

For each sample, the flame spread parameter was calculated with the values of thermal inertia by multiplying the density, specific heat and the thermal conductivity. Two values of the thermal inertia were obtained with the results of the thermal conductivity found in the previous section for side PP1, at ambient ($20 \text{ }^\circ\text{C}$) and at elevated temperatures (averaging results obtained for 30 to $225 \text{ }^\circ\text{C}$).

Table 3 shows the results of the flame spread parameter associated to each thermal conductivity. The value used for total heat transfer was $37 \text{ W/m}^2\text{K}$ following the regression proposed by Hidalgo [22]. The average value of the flame spread parameter (ϕ) for sample type B was found to be $5.41 \pm 5.45 \text{ kW}^2/\text{m}^3$, and $9.83 \pm 9.89 \text{ kW}^2/\text{m}^3$ for ambient and elevated temperatures, respectively. The average value of the flame spread parameter for sample type C was found to be $7.68 \pm 0.30 \text{ kW}^2/\text{m}^3$ and $13.57 \pm 0.53 \text{ kW}^2/\text{m}^3$ for the thermal conductivity at ambient and at the higher temperatures, respectively.

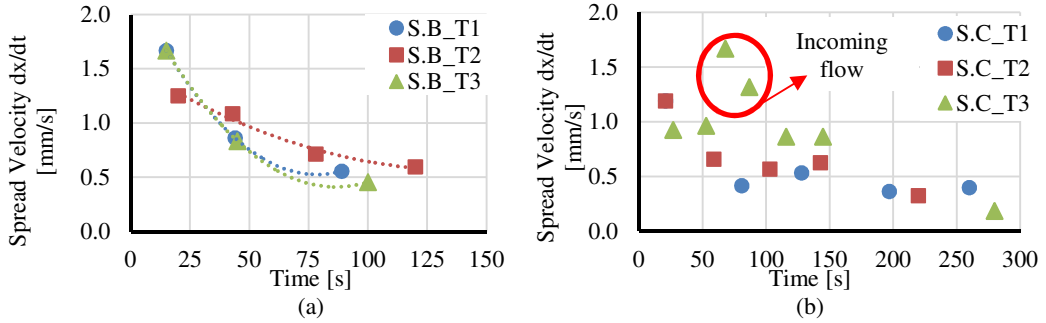


Fig. 7. Flame spread test spread velocity in time (a) sample type B (b) sample type C.

A linear regression representing Eq. (5) was used to obtain the flame spread parameter for each sample (Fig. 8).

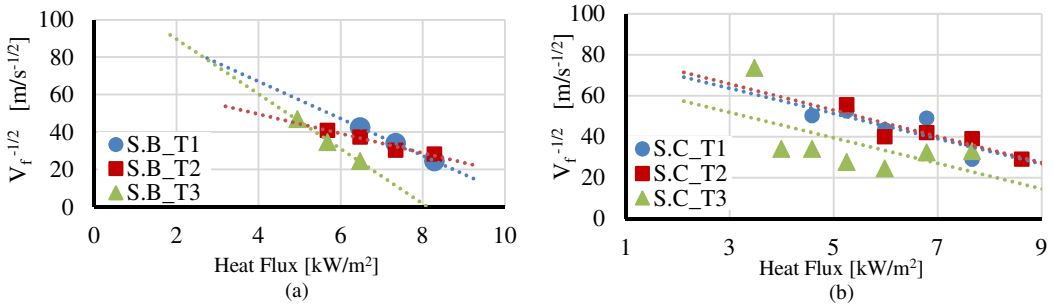


Fig. 8 Correlating plot for flame spread parameter (a) sample type B (b) sample type C.

It can be observed the high variability for sample type B, however eliminating sample S.B_T2 from the average the results obtained are $2.31 \pm 1.27 \text{ kW}^2/\text{m}^3$, and $4.196 \pm 2.21 \text{ kW}^2/\text{m}^3$ for the thermal inertia calculated with the thermal conductivity at ambient and at higher temperatures, respectively. More experiments need to be carried out to be able to validate these data.

Table 3. Flame spread parameter results of laminated bamboo “Moso” tested

Sample	ϕ with $k_{Ambient}$, kW^2/m^3	ϕ with $k_{Elevated Temp}$, kW^2/m^3
S.B_T1	3.17	5.76
S.B_T2	11.62	21.10
S.B_T3	1.45	2.63
S.C_T1	7.94	14.04
S.C_T2	7.35	13.00
S.C_T3	7.74	13.68

To the best knowledge of the authors, there is no available flame spread parameter data to compare with laminated bamboo on this subject. For charring materials, there is also limited data to compare for flame spread. According to Di Blasi [23], these types of fuels create a complex problem because of the strong interaction between the chemical processes. Atreya [24] mentioned that many of the experiments that have been made on wood are not very reproducible, due to the characteristics of wood, such as evaporation of moisture, grain direction, degradation of wood, among others.

The flame spread parameter was found for various materials by Merryweather et al. [25]. Some of the charring materials tested in this group were plywood, medium density fibreboard. Results yielded a flame spread parameter of $28.0 \text{ kW}^2/\text{m}^3$, and $17.1 \text{ kW}^2/\text{m}^3$, respectively. Both of these results show higher values to the ones obtained for laminated bamboo. However, the authors want to clarify that this is a work in progress and any comparison made to this point is to give some initial perspective on how this material stands. Nevertheless, further analysis needs to be done to completely understand the flame spread behaviour on laminated bamboo.

SUMMARY AND CONCLUSIONS

Tests have been undertaken to determine the risk of flame spread in laminated bamboo samples. For these tests, an experimental calculation of the thermal inertia was provided with the actual test measurement of the thermal conductivity.

Two different sensors were used to measure the thermal conductivity: a Kapton sensor used at ambient temperature and a Mica sensor used at elevated temperatures. Thermal conductivities provided by both sensors around ambient temperature were slightly different. Further tests will be performed to determine if the type of sensor affected the measurement at ambient temperature.

The thermal conductivity was tested at ambient temperatures (20-25 °C) as well as for higher temperatures (30-350 °C). The samples were tested perpendicular to the grain (PP1 and PP2) as well as parallel to the grain (PPL).

The sample type with the lower density (Sample A) had the lower thermal conductivity for ambient temperatures yielding a value of $0.2094 \pm 0.0057 \text{ W/mK}$. The results for Sample B and C were similar among them for the configuration perpendicular to the grain; however, the samples tested parallel to the grain depicted a slightly higher thermal conductivity.

The tests carried out at elevated temperatures and done perpendicular to the grain (PP1) showed to have a higher value than those at ambient. The results also show that the thermal conductivity displays a steady tendency up to around 225°C. Nevertheless, it starts to decrease after the samples were heated beyond 225 °C.

Experiments were carried out to find the behaviour of the spread of the flame. Samples B and C were tested perpendicular to the grain (PP1). During the preheating time, the first 250 mm of the sample degraded and charred. Once ignition started, the flame travelled around 200 mm and then quenched, at the distance where the radiative incident heat flux was around $5 \text{ kW}/\text{m}^2$.

It was observed that the maximum travelled distance recorded was around 450mm, after this extinction always occurred which resulted in a critical heat flux for flame spread of around $5 \text{ kW}/\text{m}^2$.

The average value of the flame spread parameter for sample type C was found to be $7.68 \pm 0.30 \text{ kW}^2/\text{m}^3$ and $13.57 \pm 0.53 \text{ kW}^2/\text{m}^3$ associated with the thermal conductivity at ambient and at the higher temperatures.

The flame spread parameter results for sample B showed that test S.B_T2 was out of the trend observed for the other two tests. However eliminating sample S.B_T2 from the average the results

obtained are $2.31 \pm 1.27 \text{ kW}^2/\text{m}^3$, and $4.196 \pm 2.21 \text{ kW}^2/\text{m}^3$ for the thermal conductivity at ambient and higher temperatures, respectively.

It can be observed the high variability for sample type B, so more experiments need to be carried out to be able to validate these data, and further analysis needs to be considered to completely understand this condition.

ACKNOWLEDGEMENTS

Non-financial support to this research was provided by several individuals and companies and we would like to highlight in particular Moso International and Yes Bamboo. The authors gratefully acknowledge The University of Queensland's Centre for Future Timber Structures for its support throughout this research; as well as Dr Andres Osorio, Jeronimo Carrascal, Dr Cristian Maluk, Mateo Gutierrez, Ian Pope, Aaron Bolanos, Tam Do, and the rest of the UQ Fire Research Team for their feedback and motivation.

REFERENCES

- [1] X. Liu, et al., Nomenclature for Engineered Bamboo, *BioResources*, 11 (2016) 1141-1161.
- [2] L. Yiping, et al., Bamboo and climate change mitigation. Technical Report-International Network for Bamboo and Rattan (INBAR), Vol. 32, 2010.
- [3] P. Van der Lugt, A.A.J.F. Van den Dobbelsteen, J.J.A. Janssen, An environmental, economic and practical assessment of bamboo as a building material for supporting structures, *Construct. Build. Mater.* 20(9) (2006) 648-656.
- [4] B. Sharma, et al., Engineered bamboo for structural applications, *Construct. Build. Mater.* 81 (2015) 66-73.
- [5] A. Gatóo, et al. Sustainable structures: bamboo standards and building codes, In: *Proceedings of the Institution of Civil Engineers-Engineering Sustainability*, Thomas Telford Ltd., 2014.
- [6] Y. Hasemi, Surface flame spread, In: *SFPE Handbook of Fire Protection Engineering*, Springer, 2016, pp. 705-723.
- [7] J.L. Torero, Scaling-up fire, *Proc. Combust. Inst.* 34 (2013) 99-124.
- [8] J. Torero, Flaming ignition of solid fuels, In: *SFPE Handbook of Fire Protection Engineering*, Springer, 2016, pp. 633-661.
- [9] T.L. Bergman, A.S. Lavine, F.P. Incropera, D.P. DeWitt, *Fundamentals of heat and mass transfer*, John Wiley & Sons, 2011.
- [10] B. Sharma, et al., Engineered bamboo: state of the art, *Proc. Inst. Civil Eng. – Construct. Mater.* 168(2) (2015) 57-67.
- [11] C. Fernandez-Pello, T. Hirano, Controlling mechanisms of flame spread, *Combust. Sci. Technol.* 32 (1983) 1-31.
- [12] H.D. AB, *Hot Disk Thermal Constants Analyser Instruction Manual*, 2015.
- [13] M. Gustavsson, E. Karawacki, S.E. Gustafsson, Thermal conductivity, thermal diffusivity, and specific heat of thin samples from transient measurements with hot disk sensors, *Rev. Sci. Instr.* 65 (1994) 3856-3859.
- [14] J. De Ris, Spread of a laminar diffusion flame, *Proc. Combust. Inst.*, 12 (1969) 241-252.
- [15] J. Quintiere, The application of flame spread theory to predict material performance, *J. Res. National Bureau of Standards* 93 (1988) 61-70.
- [16] D. Drysdale, *An introduction to fire dynamics*, John Wiley & Sons, 2011.
- [17] J. Quintiere, A simplified theory for generalizing results from a radiant panel rate of flame spread apparatus, *Fire Mater* 5 (1981) 52-60.

- [18] ASTM E1321-13 Standard Test Method for Determining Material Ignition and Flame Spread Properties, E.F. Standards, ASTM, 2009.
- [19] A. Solarte, J.P. Hidalgo, J.L. Torero, Flammability Studies for the Design of Fire-Safe Bamboo Structures, In: World Conference on Timber Engineering, Seoul, Republic of Korea, 2018.
- [20] A.I. Bartlett, et al., Thermal and Flexural behaviour of Laminated Bamboo exposed to sever radiant heating, In: World Conference on Timber Engineering, Seoul, Republic of Korea, 2018.
- [21] D.U. Shah, et al., Thermal conductivity of engineered bamboo composites, *J. Mater. Sci.* 51 (2016) 2991-3002.
- [22] J.P. Hidalgo, Performance-based methodology for the fire safe design of insulation materials in energy efficient buildings, the University of Edinburgh, 2015.
- [23] C. Di Blasi, Processes of flames spreading over the surface of charring fuels: effects of the solid thickness, *Combust. Flame* 97 (1994) 225-239.
- [24] A. Atreya, Fire growth on horizontal surfaces of wood, *Combust. Sci. Technol.* 39 (1984) 163-194.
- [25] G. Merryweather, M. Spearpoint, Flame spread measurements on wood products using the ASTM E 1321 LIFT apparatus and a reduced scale adaptation of the cone calorimeter, *Fire Mater* 34(3) (2010) 109-136.